Experimental determination of line-intensity ratios for the $n=3$ to $n=2$ transitions of O V, F VI, and Ne VII at electron densities in a range of $(4-9)\times 10^{12}$ cm^{-3}

L. K. Huang, S. Lippmann, B. C. Stratton,* and H. W. Moos
Department of Physics and Astronomy, The Johns Hopkins University, Baltimore, Maryland 21218

M. Finkenthal
Racah Institute of Physics, Hebrew University, Jerusalem, Israel
(Received 25 September 1987)

This paper reports relative-line-intensity measurements of the $n=3$ to $n=2$ transitions for O V, F VI, and Ne VII in an electron density range of $(4-9)\times 10^{12}$ cm^{-3} in a tokamak plasma. Large discrepancies were found between the experimentally measured and theoretically computed values. The discrepancies are due to inaccuracies in the computations of the electron collision strengths from the $2s^2$ and $2s2p$ levels to the $2s3p$ levels, using either the R-matrix method or the distorted-wave approximation.

I. INTRODUCTION

The $n=3$ to $n=2$ transitions of Be I-like O V and Ne VII have been recorded over the spectral range of 90–250 Å for solar flares,[1,2] and the line-intensity ratios of O V in these solar spectra have been studied in order to derive both the electron temperature and density of the flares.[3] Recent developments in technology will allow extreme UV astronomical studies [below 900 Å, where these $\Delta n=1$ transitions emit (see Table II)] of other stars with high spectral resolution and high sensitivity.[4,5] Therefore, these $\Delta n=1$ transition lines are potentially important diagnostics in future astrophysical studies. In magnetically confined fusion devices, the line intensity ratios of these $\Delta n=1$ transitions to the transitions within the $n=2$ complex can be very sensitive measure of the electron temperature in the edge plasma. Applications of the kind described above require reliable atomic data, and the purpose of the experiment described here was to check existing computations of the line-intensity ratios of the $n=3$ to $n=2$ transitions for the low-Z Be I-like ions.

This paper presents the measured relative intensities of spectral lines originating from the $n=3$ to $n=2$ transitions of O V, F VI, and Ne VII in plasmas of the Texas Experimental Tokamak[6] (TEXT) in an electron density range of $(4-9)\times 10^{12}$ cm^{-3}. There are other laboratory measurements on these lines, e.g., Johnston and Kunze[7] and Lang[8], using θ-pinch machines at much higher electron densities (near 10^{16} cm^{-3}). One advantage of the experiment described here compared to the θ-pinch machines is the stable, well-diagnosed tokamak plasma. However, a more important difference is the difference in the electron density, because a relatively low electron density makes the atomic model simpler, involving electron excitation of fewer transitions. This will be discussed in more detail in Sec. III.

Although line ratios were measured for O V, F VI, and Ne VII, the eligible computation results were one based on the R-matrix method for the case of O V and one based on a distorted-wave approximation for Ne VII.[3,9] A comparison of the experimental and theoretical values shows large discrepancies for several of the ratios for O V and Ne VII. These discrepancies are related to the calculated electron excitation rates to the $2s3p$ levels from the $2s^2$ and $2s2p$ levels for both the R-matrix method and the distorted-wave approximation.

II. EXPERIMENT

The experiment was conducted using the TEXT.[6] The tokamak plasma had a major radius of 100 cm and a minor radius of 27 cm. The discharge lasted 600 msec with a plateau of 400 msec. The line average electron density was set at 3.5×10^{13} cm^{-3}, and the plasma central electron temperature was 1 keV. Figure 1 presents the electron density and temperature profiles near the plasma edge, where shells of the low-Z Be I-like ions were concentrated. These profiles were measured using Langmuir probes at the edge and then extrapolated to the central plasma by requiring consistency with the far-infrared interferometry measurements for the density and with the Thomson scattering measurements for the temperature.

The spectra of Ne VII, F VI, and O V were recorded using a grazing-incidence time-resolving spectrograph[10] (GRITS), which viewed the plasma torus along a major radius. It simultaneously covers a band from 40 to 80 Å over the spectral range of 15–360 Å. The spectral resolution is 0.7 Å. The wavelength calibration uncertainty is 0.2 Å. A photoelectric detector of 1024 pixels integrates incoming signals for a period of 5.4 msec and is continuously scanned 32 times during each tokamak discharge. Each scan records a complete spectrum.

The GRITS was photometrically calibrated using synchrotron radiation at the National Bureau of Standards. Because the spectral lines of a given ion were close to each other in wavelength and were measured within a central region of the detector where the photometric calibration is reliable, the relative photometric calibration uncertainty is $\pm 5\%$.[11] Both lines for a given line ratio

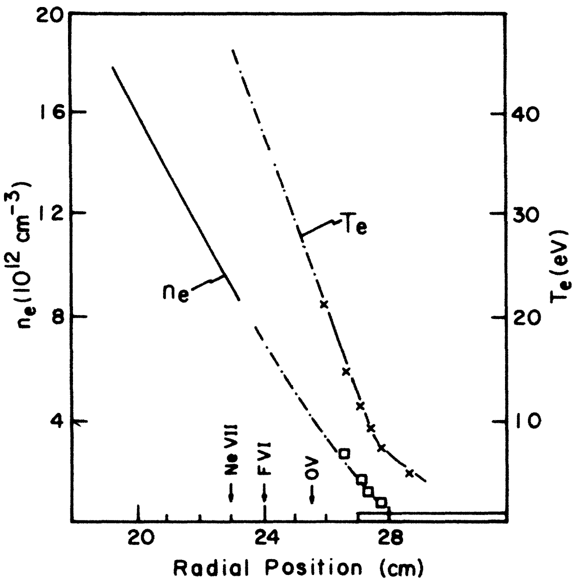

FIG. 1. Electron density n_e and temperature T_e near the edge of the TEXT plasma. The emission peak positions of the Be I-like ions are indicated with arrows. The limiter was at 27 cm away from the center.

TABLE I. Plasma properties.

Ions	O V	F VI	Ne VII
r^a(cm)	25.5±1	24±1	23±1
n_e (10^{12} cm^{-3})	4±2	7±2	$9\pm\frac{5}{2}$
T_e (eV)	26±9	37±10	47±10
T^b_{equ} (eV)	20	31	47

[a] r: minor radius of the peak of emission shell.
[b] T_{equ}: ionization equilibrium temperatures, Refs. 13 and 14.

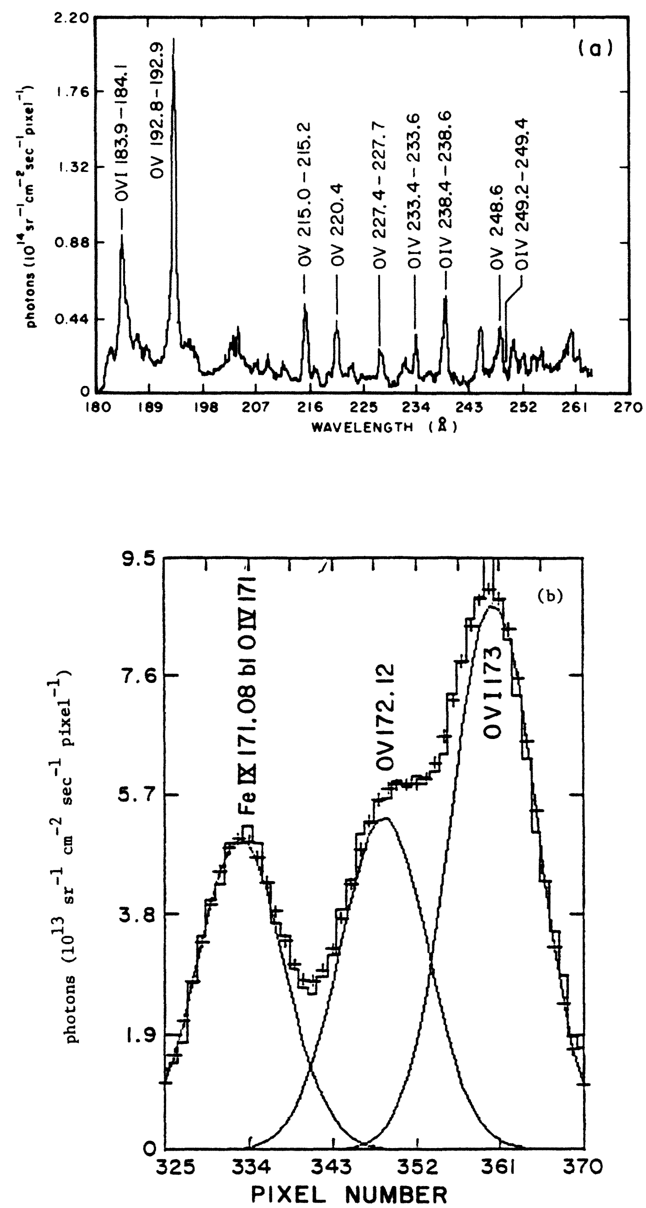

FIG. 2. (a) Emission spectrum of O V from the edgy plasma of the TEXT. (b) Determination of the intensity of the O V 172-Å feature using the Gaussian fitting procedure. The histogram is the data and the + symbols are the sum of the Gaussian fitting. The pixel is a unit in the photodiode array.

were measured in a single shot. Therefore, the shot-to-shot variations of the plasma did not affect the measurements. The uncertainty of the measured line ratios was mainly due to the background emission noise, which will be examined later for each spectrum.

Radial profiles of the line brightness were provided by scanning radially on a shot-to-shot basis. The spatial resolution of the spectrograph was 2 cm. The emission profiles were obtained via Abel inversion.[12] The bulk emission came mainly from a shell about 2 cm thick full width at half maximum (FWHM) and emission peak locations are marked in Fig. 1. The electron density and temperature at the emission peak are determined from Fig. 1 and are listed in Table I. The ionization equilibrium temperature T_{equ} is listed for comparison.[13,14] The uncertainty in the determination of both electron density and temperature and the relative consequence in the line intensity ratios will be discussed for the O V and the Ne VII cases below.

The measured and predicted relative intensities of the $n=3$ to $n=2$ transition lines for O V, F VI, and Ne VII are listed in Table II. Details of the measurements are given in Secs. II A, II B, and II C, respectively, for each ion. The experimental details are then followed by comparisons of the measured line ratios with the predicted ones.

A. O V

Oxygen is an intrinsic impurity in the tokamak. The line of sight of the GRITS intersected the edge plasma shells at a near tangent. As a consequence, the O V lines were very bright and prominent, and the background emissions from high ionization potential ions (which are

TABLE II. Relative emission intensities.

Ions Transitions		O V λ (Å)	O V I_{meas}/I^{a}_{calc}	F VI λ (Å)	F VI I_{meas}/I_{calc}	Ne VII λ (Å)	Ne VII I_{measu}/I^{b}_{calc}
$2s2p\ ^3P-2s3d\ ^3D$		192.8–192.9	1.00/1.00	139.8–139.9	1.00	106.0–106.2	1.00/1.00
$2s2s\ ^1S-2s3p\ ^1P$	R_1	172.2	0.29[c]/0.13	126.9	0.23[c]	97.5	0.31[c]/0.13
$2s2p\ ^3P-2s3s\ ^3S$	R_2	215.0–215.2	0.29[d]/0.56	153.7–153.9	0.30[d]	115.3–115.5	0.30[d]/0.17
$2s2p\ ^1P-2s3d\ ^1D$	R_3	220.4	0.23[d]/0.23	156.2	0.29[d]	116.7	0.31[d]/0.37
$2p2p\ ^3P-2p3s\ ^3P$	R_4	227.4–227.7	0.14[e]	161.2–161.5	0.20[e]	120.2–120.5	0.27[e]
$2s2p\ ^1P-2s3s\ ^1S$	R_5	248.6	0.19[e]/0.24	173.1	0.20[f]	127.7	0.24[f]/0.28

[a]The calculated line intensity. Note that the collision strengths for $\Delta n=1$ transitions were calculated using the R-matrix method, Ref. 3.
[b]The calculated line intensity. Note that the collision strengths for $\Delta n=1$ transitions were obtained by the distorted-wave approximation and the Born approximation, Ref. 9.
[c]A fitted line with an uncertainty less than 26%.
[d]Accurate measurement with an uncertainty less than 15%.
[e]Uncertainty of 20%.
[f]A blended line with an uncertainty of 65% (see the text).

present only in the central plasma) was small (see Fig. 2). Thus the uncertainty in the measured line intensity was small. The measured line intensities in Table II were normalized to those of the brightest transitions, $2s2p\ ^3P-2s3d\ ^3D$. The total uncertainty in the measured relative line intensity of the $2s2p\ ^3P-2s3s\ ^3S$ transition at 215 Å was 15%, and the relative intensities of the $2p^2\,^3P-2p3s\ ^3P$ transitions at 227 Å and the $2s2p\ ^1P-2s3s\ ^1S$ transitions at 249 Å had only slightly larger uncertainties of 20%. The O V 172.17-Å line of the $2s^2\,^1S-2s3p\ ^1P$ transition was near strong emissions of O VI 173-Å lines, O IV 171-Å and Fe IX 171-Å lines on each side, as shown in Fig. 2(b). A Gaussian line shape fitting procedure was used to deconvolute these lines.[11] (The intensity of the O V 171.6-Å lines of the $2s^2\,^1S_0-2s3p\ ^3P_1$ transitions was assumed to be negligible compared to its neighbors, as theoretical calculations indicated that the total emissivity of these lines is about 10% of the O V 172-Å line intensity.[3,15]) The resulting total uncertainty in the O V 173-Å line intensity determined by the fitting procedure was less than 25%, and the uncertainty in the line ratio was 26%.

The O V line ratios in Table II were computed using the effective electron collision strengths based on the R-matrix method,[3,16] and the radiative transition rates including configuration interactions and relativistic corrections.[15] Twenty levels in configurations of $2l2l'$ and $2s3l$ were included in the corona equilibrium equations. Both the electron collisional excitations to $n=3$ levels from levels higher than $2s2p\ ^1P$ and the proton collisions were ignored. In those cases where the computed ratios were also listed in Ref. 3, the agreement was within 10%.

Two measured line intensity ratios,

$$I(2s2p\ ^1P-2s3d\ ^1D)/I(2s2p\ ^3P-2s3d\ ^3D)$$

and

$$I(2s2p\ ^1P-2s3s\ ^1S)/I(2s2p\ ^3P-2s3d\ ^3D)\ ,$$

were in very good agreement with the computed values. However, large discrepancies were found between the measured and predicted values of the ratios

$$R_1=I(2s^2\,^1S-2s3p\ ^1P)/I(2s2p\ ^3P-2s3d\ ^3D)$$

and

$$R_2=I(2s2p\ ^3P-2s3s\ ^3S)/I(2s2p\ ^3P-2s3d\ ^3D)\ .$$

The experimental value for R_1 was 123% larger than the prediced value, and for R_2, 48% smaller. These discrepancies are much larger than the uncertainties in the measured line-intensity ratios. Note that the degree to which particular transitions of measured relative line intensity appear to agree or disagree with the theoretical calculation depends on the transition chosen for the denominator in the ratio. In fact, the one chosen gives the fewest number of lines with a discrepancy.

The uncertainties in the determination of both the electron density and the temperature cannot explain these large discrepancies. The lower bounds of the electron density and temperature were 2×10^{12} cm^{-3} and 2×10^5 K, and the upper bounds 6×10^{12} cm^{-3} and 4×10^5 K, respectively. As shown in Fig. 3, if the actual plasma conditions were at the lower bounds, the discrepancies would, in fact, have been larger. At the upper bounds, the computational results changed by only 5% or less, which would not be large enough to meet the discrepancies.

B. Ne VII

Neon was introduced into the tokamak by using gas-puffing through a fast valve.[17] The spectra was used for this study were taken when the Ne VII line emissions rose to a maximum, and the Ne VII lines were very bright. In addition, a background emission spectrum obtained before the neon puffing was subtracted. (The standard techniques for the background noise reduction and line identification, such as the background subtraction, the spatial location, and time history of line emissions used in our tokamak, and mirror studies, are described elsewhere.[11,18]) Thus the neon lines in the resulting spectra were well separated from most of the other intrinsic impurity lines.

The Ne VII 115-Å line was near the O VI 115.8-Å lines of the $2s\,^2S-4p\,^2P$ transitions. In order to estimate the residue of the O VI line after the spectral subtraction, other O VI lines emitted from $n=3$ and $n=4$ levels, at 150 Å, 173 Å, and 130 Å, were monitored. The intensity fluctuation of these lines was less than 5% during the gas-puffing. The O VI 115.8-Å line intensity prior to injection was 50% of the Ne VII 115-Å line intensity after injection. Thus, after the background subtraction, the O VI line signal was largely eliminated, and the uncertainty in the measured Ne VII line intensity due to O VI was less than 3%. The total uncertainty of the relative intensity of Ne VII 115 Å is less than 15%.

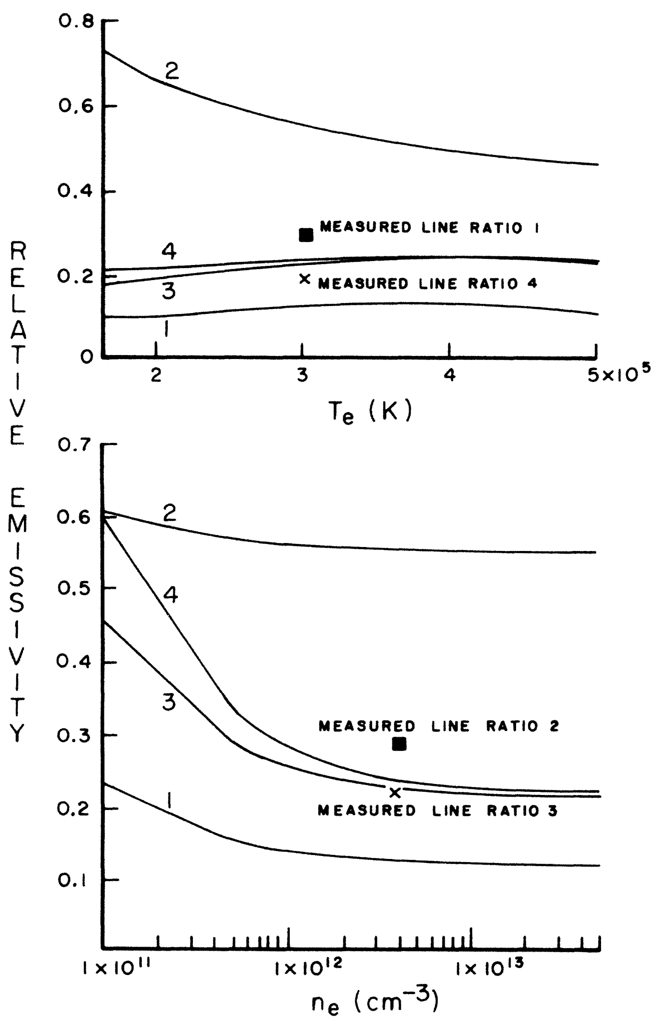

FIG. 3. Computed O V line intensities relative to the $2s2p\,^3P-2s3d\,^3D$ line intensity as a function of electron density and temperature. The ratios are insensitive over the range of possible plasma conditions for this study. The numbered lines correspond to the following transitions: (1) $2s^2\,^1S-2s3p\,^1P$, (2) $2s2p\,^3P-2s3s\,^3S$, (3) $2s2p\,^1P-2s3d\,^1D$, (4) $2s2p\,^1P-2s3s\,^1S$. The upper figure is for an electron density of 4×10^{12} cm^{-3}. The lower figure is for an electron temperature of 3×10^5 K. The measured line ratios 3 and 4 were in good agreement with the computed values, but the measured line ratios 1 and 2 differ by a factor of 2 from the computed values.

Another blending problem occurred between the $2s2p\,^1P-2s3s\,^1S$ transition at 127.7 Å and a Ne VI $2s2p^2\,^2P_{3/2}-2s2p3d\,^3P_{3/2}$ transition at 127.8 Å. In order to estimate the Ne VII 127.7-Å intensity, the line ratios $R_5=I$(Ne VII 128 Å)/I_5(Ne VII 106 Å) and $r=I$(Ne VI 128 Å)/I_r(Ne VI 122 Å) were approximated as constant across the emission shell at a minor radius of 23 cm, and thus the total measured intensity of the blended lines at 128 Å was $I_b=rI_r+R_5I_5$. We measured two sets of I_b, I_r, and I_5 through the chords at 22 and 24 cm, respectively. Substituting these two sets of intensity values into the equation for I_b, I_r, and I_5, and solving the simultaneous linear equations for the line ratios, we found $R_5=0.24$ and $r=0.08$. It is difficult to estimate the uncertainty in the derived R_5. However, the upper limit of the uncertainty may not exceed 65% if the variation of r and R_5 across the emission shell is negligible.

The $2s^2\,^1S-2s3p\,^1P$ transition line at 97.5 Å was separated from the Ne VIII 98.3-Å line by using the Gaussian line shape fitting procedure, as in the case of O V. (The intensity of the blended Ne VII line of the transition $2s^2\,^1S_0-2s3p\,^2P_1$ at 97.3 Å is estimated to be less than 8% relative to the one at 97.5 Å. This estimate was obtained by examining the Ne VII $2s3p\,^3P-2p^2\,^3P$ at 135.5 Å, which was also blended. The upper limit for the intensity including the blended was 0.12 relative to the $2s2p\,^3P-2s3d\,^3D$ line. Then, using calculated branching ratios and level population ratios of the $2s3p\,^3P$,[9] we obtained the upper limit for the value at 97.5 Å. (The upper bound of Ne VII is much smaller than the result directly from Ref. 9.) The total uncertainty in the measured relative line intensity at 97.5 Å was 26%.

The computed line ratios in Table II were taken from Ref. 9, which included 20 levels in the $2l2l'$ and $2s3l$ configurations. The electron collision strengths used in that calculation were computed using different approximations: the R-matrix method only for transitions within $n=2$ levels, the distorted-wave approximation for transitions to the $2s3l$ levels from $2s^2$ and $2s2p$ levels, and the Coulomb-Born exchange calculations for transitions to $2s3l$ levels from the $2p2p$ levels to the $2s3l$ levels. No calculations of electron collisions strengths within the $n=3$ levels are available, but as will be discussed in Sec. III, these transitions are negligible at tokamak lower densities.

Two measured line intensity ratios, $I(2s2p\,^1P$ $2s3d)/I(2s2p\,^3P-2s3d\,^3D)$ and $I(2s2p\,^1P-2s3s\,^1S)/I(2s2p\,^3P-2s3d\,^3D)$, were in good agreement with the computation. Once again, large discrepancies between the computed and the measured values were found; those for R_1 differed by 138% and for R_2 by 76%, respectively. The same comment made for O V about the choice of the denominator also holds here.

During the neon gas-puffing, the electron density increased by 27%, and the electron temperature might be overestimated. Changing the electron temperature and density within the uncertainty of the measurements lead to changes in the computed line ratio R_2 of only 7% or less, which is much smaller than the discrepancy mentioned above. The computed value of R_1 could be increased by not more than 20%, which is not enough to meet the discrepancy, by assuming the lower limit of the electron density or the upper limit of the electron temperature. In fact, during the Ne gas-puffing, the density increased and temperature decreased, which will decrease rather than increase R_1.

C. F VI

F VI spectra were studied as a complement to the O V and Ne VII studies. Although no theoretical calculations are available for comparison, with these three elements one can check trends in the intensity ratios along the isoelectronic sequence in order to judge the correctness of both the line identifications and the intensity measurements.

Fluorine was introduced into the tokamak by puffing in SF_6 gas. In a manner analogous to Ne VII, spectra at the F VI emission peak were used and a spectrum obtained before gas-puffing was subtracted in order to suppress the intrinsic element emission background.

The measured relative line intensities of these F VI lines in Table II are comparable with those for Ne VII. The relative line intensity of the $2s^2\,{}^1S-2s3p\,{}^1P$ transition was estimated with a 25% uncertainty, using the fitting procedure as in the case of O V. The $2s2p\,{}^1P-2s3s\,{}^1S$ line at 173.1 Å was treated with the same method as the Ne VII line at 127.7 Å.

Each measured line ratio of F VI shows a tendency consistent with the experimental results for O V and Ne VII, giving the confidence that there are no apparent mistakes either in the line identifications or the intensity measurements.

III. DISCUSSION

The comparison between the experimental and the computed line-intensity ratios displayed in Table II shows the large discrepancies in level populations for both O V and Ne VII. As discussed previously for the case of O V, the choice of the $2s2p\,{}^3P-2s3d\,{}^3D$ transitions as the denominator for the line-intensity ratios minimizes the number of levels which show a discrepancy. In addition, there is also a theoretical consideration for choosing this transition, i.e., both the R-matrix method and the distorted-wave calculations give very close values for the collision strengths of the dominant transitions from the $2s^2$ and $2s2p$ levels to the $2s3d\,{}^3D$ levels.[3] Thus for both O V and Ne VII the experimental results imply that large inaccuracies exist in the computed values of the collision strengths which control the populations of the $2s3s\,{}^3S$ for the case of R_2 and $2s3p\,{}^1P$ for the case of R_1.

The atomic data used in the level population calculations can be separated into two portions, the transitions within $n=2$ complex and the transitions involving $n=3$ levels. A recent experiment confirmed the reliability of the R-matrix method for computations of the electron collision strengths within the $n=2$ complex of low-Z Be I-like ions.[19] Thus the present experiment tests the results for transitions involving the $n=3$ levels.

In order to relate the sensitivity of a given line-intensity ratio to each of the computed electron collisional excitation rates contributing to the calculated level populations, define a parameter S_{ij}^k as the ratio of the percentage change in the line ratio to a percentage increment

$$S_{ij}^k=(C_{ij}\delta R_k)/(R_k\delta C_{ij})\ ,$$

where R_k is a given line emissivity ratio and C_{ij} is a given transition rate. Thus values of S_{ij}^k for different ij give the relative importance of the different excitation rates and the sensitivity of the calculated ratios to inaccuracies in the different C_{ij}'s. The S_{ij}^k also can be rewritten as $[(C_{ij}\delta P_k)/(P_k\delta C_{ij})]-[(C_{ij}\delta P_d)/(P_d\delta C_{ij})]$, where P_k is the upper-level population in the numerator of R_k and P_d is the upper level population of $2s3d\,{}^3D$ in the denominator. Because there are no significant radiative transitions from the $2s3d\,{}^3D$ levels to the other $n=3$ levels and, as discussed in the next paragraph, collisional transitions from the $2s3d\,{}^3D$ to the other $n=3$ levels are negligible at tokamak densities, S_{ij}^k is equal to either $(C_{ij}\delta P_k)/(P_k\delta C_{ij})$ or $-(C_{ij}\delta P_d)/(P_d\delta C_{ij})$ for the $2l2l'-2s3l$ transitions. Therefore S_{ij}^k is equivalent to the fractional contribution to the level population due to the ij transition. We have calculated S_{ij}^k for a number of transitions of O V and Ne VII over the electron density range from 1×10^9 to 1×10^{16} cm^{-3} using published atomic data.[3,15,16,20–22] The more important values of S_{ij}^k for R_1 and R_2 in O V, which are based on the R-matrix method calculation of electron collision strengths, are presented in Fig. 4. Table III lists the associated energy levels and labels.

Although the calculations of R_k and S_{ij}^k included all of the transitions within the $n=2$ complex and the transitions between the first four levels and $2s3l$ levels, no transitions from levels above the $2s2p\,{}^3P$ levels to the $2l3l'$ levels were included. Computed values of these excitation rates are not available and were set equal to zero in our calculation, as they were judged to be important only at higher densities. To estimate their relative importance we have computed $(\delta R_k/\delta C_{ij})/R_k$. The values presented in Fig. 5 for R_1 have been multiplied by 1×10^{-9}, a typical large excitation rate for these ions, to provide a rough estimate of their contribution. It is clear from the figure that below an electron density of 3×10^{14} cm^{-3} the effects of these transitions are negligible, an advantage for the studies performed at tokamak densities which are lower than θ-pinch densities. A similar conclusion was obtained for R_2. (As the derivative $\delta R_k/\delta C_{ij}$ was evaluated near $C_{ij}=0$, the linear approximation may not be hold at very high densities, and the values should be used as indicative.)

Figures 4 and 5 show that for the low-Z Be I-like ions studied in this paper, the electron density can be divided into three regions. Below 1×10^{11} cm^{-3}, the $n=3$ levels are predominately populated by electron impact excitations from the ground state, $2s^2\,{}^1S$. In the range from 1×10^{11} to 3×10^{14} cm^{-3}, the excitations to the $n=3$ levels from the $2s2p\,{}^3P$ levels become important, but those from levels higher than $2s2p\,{}^3P_2$ are negligible. Beyond

TABLE III. Energy levels of O v.

No.	Term	Wave number (cm^{-1})
1	$2s2s\ ^1S_0$	0
2	$2s2p\ ^3P_0$	819 39
3	$2s2p\ ^3P_1$	820 75
4	$2s2p\ ^3P_2$	823 82
5	$2s2p\ ^1P_1$	158 798
6	$2p2p\ ^3P_0$	213 459
7	$2p2p\ ^3P_1$	213 615
8	$2p2p\ ^3P_2$	213 884
9	$2p2p\ ^1D_2$	231 721
10	$2p2p\ ^1S_0$	287 910
11	$2s3s\ ^3S_1$	546 969
12	$2s3s\ ^1S_0$	561 276
13	$2s3p\ ^1P_1$	580 825
14	$2s3p\ ^3P_0$	582 803
15	$2s3p\ ^3P_1$	582 840
16	$2s3p\ ^3P_2$	582 917
17	$2s3d\ ^3D_1$	600 746
18	$2s3d\ ^3D_2$	600 756
19	$2s3d\ ^3D_3$	600 766
20	$2s3d\ ^1D_2$	612 616

3×10^{14} cm^{-3}, none of these excitations can be ignored.

The effects of cascades from higher levels on the $2s3l$ levels were not included in the level population model. The effects of direct cascades from $2p3l$ levels to the $2s3l$ levels can be ignored because the radiative transition rates for $2s3l$-$2p3l$ are much smaller than those for $2l2l'$-$2p3l$.[15] Evidence for cascades from the $n=4$ levels was also searched for in this experiment. The $n=4$ to $n=2$ transitions of O v emit lines in the range from 100 to 200 Å, within the sensitive range of the GRITS. No strong lines from the $n=4$ levels could be identified. The radiative transition probabilities from $n=4$ to $n=3$ were estimated to be slightly smaller than that from $n=4$ to $n=2$. Thus the cascades from the $n=4$ levels to the $2s3l$ levels can be ignored. The effect of cascades on the $n=2$ levels is also very small because the population rate in these high levels is much smaller than the rates between the $n=2$ levels. In conclusion, the 20-level model used was adequate for accurate calculations of the R_k.

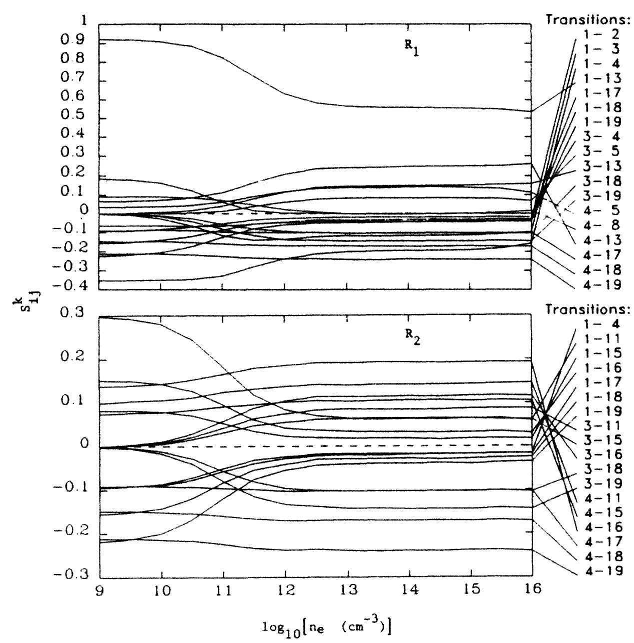

FIG. 4. More important values of $S_{ij}^k=(C_{ij}\delta R_k)/(R_k\delta C_{ij})$ for R_1 and R_2 of O v as a function of n_e. The numbers on the right side of the figures label the levels of the transitions as listed in Table III. An electron temperature of 26 eV is assumed.

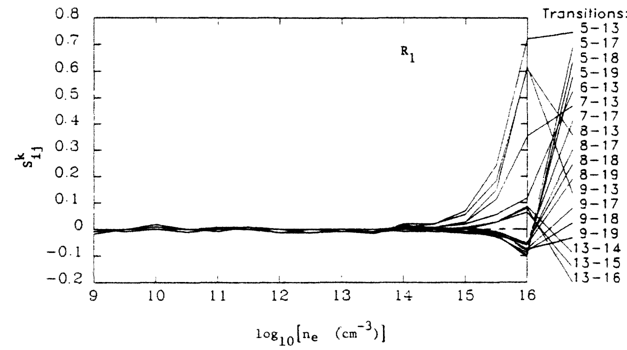

FIG. 5. Quantity $(\delta R_1/\delta C_{ij})/R_1$ for transitions from levels higher than $2s2p\ ^3P_2$ is plotted to indicate at which electron densities these transitions are negligible. The values have been multiplied by 1×10^{-9}, a typical large excitation rate.

The simplicity of the model makes it possible to examine directly a few of the important electron collisional transition rates from the $2s^2\ ^1S$ and $2s2p\ ^3P$ levels to $n=3$ levels. In the following analysis we determine which transitions in the collision strength calculations are likely to be in error and the degree of inaccuracy in order to explain the large discrepancies in the line ratios R_1 and R_2.

In the case of O v, the collision strengths computed by the R-matrix method were used,[3,16] which is generally regarded as more accurate then the distorted-wave approximation.[3,19,23] First, consider R_2. The collision strengths used for the transitions from the $2s^2\ ^1S$ and $2s2p\ ^3P$ to the $2s3s\ ^3S$ are a factor of 2 larger than the distorted-wave approximation results.[3,23] However, these transitions contribute only 32% of the population of the $2s3s\ ^3S$ level (see Fig. 4). Reducing the calculated electron excitation rates of $2s2l$-$2s3s\ ^3S$ by a factor of 2 decreases the calculated R_2 only by 16%. The $2s3s\ ^3S$ level primarily gains its population by radiative cascades from the $2s3p\ ^3P$ ($\sim$63%). If one assumes that the lower limit for the excitation rate for the transitions from the $2s^2\ ^1S$ and $2s2p\ ^3P$ to the $2s3s\ ^3S$ is a factor of 2 smaller than the R-matrix result, one would still have to reduce the collision strength for the $2s2p\ ^3P-2s3p\ ^3P$ by at least a factor of 2 in order to meet the experimental value of R_2. The line ratio R_1 is overwhelming due to the electron excitation of $2s^2\ ^1S-2s3p\ ^1P$ ($\sim$59%), followed by $2s2p\ ^3P-2s3p\ ^1P$ ($\sim$38%) (see Fig. 4). As the measured line ratio was a factor of 2 larger than the computed, these excitation rates appear to be underestimated b a factor of 2.

The predominant electron excitation rates from $n=2$

to $n=3$ for Ne VII were calculated by the distorted-wave approximation and were possibly underestimated, as in the case for O V. At the electron density and temperature of our experiment, the important contributions to the $2s3s\ ^3S$ level population came from the excitations of $2s2p\ ^3P-2s3p\ ^3P$ ($\sim 52\%$), including all possible (J-J'), followed by $2s^2\ ^1S-2s3s\ ^3S$ ($\sim 18\%$), $2s2p\ ^3P_2-2s3s\ ^3S$ ($\sim 12\%$), $2s2p\ ^3P_1-2s3p\ ^3P_1$ ($\sim 8\%$), and $2s^2\ ^1S-2s3p\ ^3P_2$ ($\sim 6\%$). Therefore these excitation rates also appear to be underestimatd by a factor of 2. For the ratio R_1, the excitation from $2s^2\ ^1S$ to $2s3p\ ^1P$ contributes $\sim 90\%$ of population to the $2s3p\ ^1P$ level. Thus the $2s^2\ ^1S-2s3p\ ^1P$ excitation rate is more than a factor of 2 smaller than it should be.

The levels of measured line-intensity ratios which disagree with the theoretical values are primarily populated by the electron excitations to both the $2s3p\ ^1P$ and the $2s3p\ ^3P$ levels. The difficulties in theoretical calculations of radiative transition probabilities for the $2s3p$ configuration have been discussed elsewhere.[15,21,24] The ^1P and ^3P level compositions are inverted between O V and Al X from the order given by Hund's rule because of the $2p3s$-$2s3p$ interaction.[24] This configuration interaction may affect the computations of the relative electron excitation rates for O V and Ne VII, and cause the large discrepancies between experiment and theory for the line ratios R_1 and R_2.

IV. CONCLUSION

This experiment determined the line-intensity ratios of the $n=3$ to $n=2$ transitions for the low-Z Be I-like ions at electron densities in the range of $4-9\times 10^{12}$ cm^{-3}. Two measured line intensity ratios

$$I(2s2p\ ^1P-2s3d\ ^1D)/I(2s2p\ ^3P-2s3d\ ^3D)$$

and

$$I(2s2p\ ^1P-2s3s\ ^1S)/I(2s2p\ ^3P-2s3d\ ^3D)\ ,$$

agree very well with the computation. Large discrepancies between the experiment and the computations were found in the other two line ratios,

$$I(2s^2\ ^1S-2s3p\ ^1P)/I(2s2p\ ^3P-2s3d\ ^3D)$$

and

$$I(2s2p\ ^3P-2s3s\ ^3S)/I(2s2p\ ^3P-2s3d\ ^3D)\ .$$

The discrepancies can be related to the inaccuracies in the existing computations of electron collision strengths from $2s^2$ and $2s2p$ levels to the $2s3p$ levels for the low-Z Be I-like ions, using either the R-matrix method or the distorted-wave approximation. The inaccuracy can be as big as a factor of 2 and clearly indicates the need for improved theoretical values of the collision strengths.

ACKNOWLEDGMENTS

The authors are grateful to all the staff at the TEXT group for the excellent support to this experiment. We especially appreciate the kindness of Dr. P. Phillips, Dr. P. Rhopes, and Dr. B. Richards for generously providing their diagnostics on the electron temperature and density. This work is sponsored by the U.S. Department of Energy under Contract No. DE-AC02-76ET53006 to The Johns Hopkins University and Contract No. DE-AC05-78ET53043 to the University of Texas. Also the contribution of the United States—Israel Binational Science Foundation is acknowledged by the groups at The Johns Hopkins University and Hebrew University.

*Permanent address: Princeton Plasma Physics Lab, Princeton University, Princeton, NJ 08544.

[1]K. G. Widing, Astrophys. J. **258**, 835 (1982).

[2]M. Malinovsky and L. Heroux, Astrophys. J. **181**, 1009 (1973).

[3]K. G. Widing, J. G. Doyle, P. L. Dufton, and A. E. Kingston, Astrophys. J. **257**, 913 (1982).

[4]J. L. Linsky, in New Insights in Astrophysics, Proceedings of the Joint NASA-ESA-SERC Conference, University College, London, 1986 (unpublished), p. 537.

[5]R. Cruddace, Astrophys. J. **187**, 497 (1974).

[6]K. W. Gentle, Nucl. Tech. Fus. **1**, 479 (1981).

[7]W. D. Johnson and H. J. Kunze, Phys. Rev. A **4**, 962 (1971).

[8]J. Lang, J. Phys. B **16**, 3907 (1983).

[9]A. E. Kingston, P. L. Dufton, J. G. Doyle, and J. Lang, J. Phys. B **18**, 2561 (1985).

[10]W. L. Hodge and H. W. Moos, Rev. Sci. Instrum. **55**, 16 (1984).

[11]L. K. Huang, S. Lippmann, T. L. Yu, B. C. Stratton, H. W. Moos, M. Finkenthal, W. L. Lodge, W. L. Rowan, B. Richards, P. E. Phillips, and A. K. Bhata, Phys. Rev. A **35**, 2919 (1987).

[12]H. R. Griem, *Plasma Spectroscopy* (McGraw-Hill, New York, 1964).

[13]C. Breton, C. De Michelis, and M. Mattioli, J. Quant. Spectrosc. Radiat. Transfer **19**, 367 (1978).

[14]C. Breton, C. De Michels, M. Finkenthal, and M. Mattoli, Association EURATOM—Comissariat à l'Energie Atomique sur la Fusion Report No. EUR-CEA-FC-948, 1978 (unpublished), p. 207.

[15]A. Hibbert, J. Phys. B **13**, 1721 (1981).

[16]K. A. Berrington, P. G. Burke, P. L. Dufton, and A. E. Kingston, At. Data Nucl. Data Tables **33**, 195 (1985).

[17]D. R. Terry, W. Rowan, W. C. Connolly, and W. K. Leung, in Proceedings of the Tenth Symposium on Fusion Energy, Philadelphia, 1983 (unpublished), p. 959.

[18]M. Finkenthal, R. Bell, and H. W. Moos, J. Appl. Phys. **56**, 2012 (1984).

[19]M. Finkenthal, T. L. Yu, S. Lippmann, L. K. Huang, H. W. Moos, B. C. Stratton, A. K. Bhatia, R. Bengtson, W. L. Hodge, P. E. Phillips, J. L. Porter, T. R Price, T. L. Rhods, B. Richards, C. P. Ritz, and W. L. Rowen, Astrophys. J. **313**, 920 (1987).

[20]H. Nussbaumer and P. J. Storey, Astron. Astrophys. **74**, 244 (1979).
[21]D. G. Ellis, Phys. Rev. A **28**, 1223 (1983).
[22]P. H. Sampson and S. J. Goett, At. Data Nucl. Data Tables **30**, 125 (1984).
[23]M. Malinovsky, Astron. Astrophys. **43**, 101 (1975).
[24]B. C. Fawcett, At. Data Nucl. Data Tables **30**, 1 (1984).